ISSN: 2281-1346

UNIVERSITÀ DI PAVIA
Department of Economics and Management

DEM Working Paper Series

Statistical Modelling of Downside Risk Spillovers

Daniel Felix Ahelegbey
(Università di Pavia)

 # 193 (10-20)

Via San Felice, 5
I-27100 Pavia

economiaweb.unipv.it

Statistical Modelling of Downside Risk Spillovers

Daniel Felix Ahelegbey

Department of Economics and Management, University of Pavia,
Via San Felice 7, 27100 Pavia, Italy

Abstract

We extend the extreme downside hedge methodology to model sensitivity interconnectedness of market returns to the tail risk of other markets under turbulent conditions. We derive the interconnectedness via Bayesian graph structural learning. The empirical application examines the dynamic interconnectedness among 15 major markets, including G10 economies, during turbulent times. We investigate whether downside risk connections among these major markets are merely anecdotal or provide evidence of contagion and the most central market for spillover propagation. The result shows that the Covid-19 induced downside risk connections record the highest density, suggesting stronger evidence of contagion in the coronavirus pandemic than during the financial and eurozone crisis. Central to the spillover propagation is the finding that most of the transmitters and recipients of downside risk are EU markets.

Keywords: Bayesian Inference, Centrality, Contagion, Conditional VaR, Downside Risk, Extreme downside hedge, Financial Crises, Financial Networks

JEL: C31, C58, G01, G12

1. Introduction

Increased interconnectedness among financial institutions and asset markets over time play a substantial role in the contagion often observed during turbulent times (Forbes and Rigobon, 2002; Mendoza and Quadrini, 2010). One outcome is that it causes the degree of comovements in asset markets within and across countries to increase following shocks to a major market or a group of major markets, and for the shocks to propagate to markets across countries and regions, with corresponding impacts on asset prices/returns. Therefore, a clear understanding of the nature of the networks of interconnectedness among markets is critical since it is a central condition for potential contagion (see Ahelegbey and Giudici, 2020; Battiston et al., 2012; Billio et al., 2019, 2012; Diebold and Yilmaz, 2014).

The turn of events in major financial markets across the globe, especially in developed economies during the ongoing pandemic is a reminder of how interconnectedness between markets can influence investors' decisions in their selection of assets to diversify their investment. This paper examines the effects of downside risk on stock market performance in turbulent times to draw comparisons of the novel coronavirus pandemic to previous crises like the early 2000's financial market disruptions due to the dotcom bubble and September 11, the global financial crisis of 2007–2009, and the European sovereign debt crisis of 2010–2013.

We study the sensitivity of stock market performance to the downside risk of other major world markets under severe conditions. It is well known that in turbulent times some

Email address: danielfelix.ahelegbey@unipv.it (Daniel Felix Ahelegbey)

assets/markets usually perform badly while others have mild reactions. Many assets that react mildly are often desirable and usually, sell at a premium. We formalize the downside risk reaction via an extreme downside hedge (EDH) model (see Ahelegbey et al., 2020; Harris et al., 2019; Mojtahedi et al., 2020). The EDH is a parametric measure of the sensitivity of a stock's return to downside risk in the market and/or other competing stocks (Ahelegbey et al., 2020). We summarize the downside reactions among major stock markets via a network model - the use of graphs to represent statistical relationships (Lauritzen, 1996). The network summarizes the complex channels of reactions by using nodes to represent companies and edges to describe the statistical relationships between pairs of companies. By ranking companies via network centrality measures, we identify the safest from the riskiest companies, as well as the "transmitters" and "receivers" of risk in a downturn.

In modeling financial contagion via networks, the underlying structure of interactions is often unknown and must be estimated from observed data. This is related to (graph) structural learning problem. To infer networks from multivariate financial time series, the widely applied competing methods include: Granger-causality (Billio et al., 2012); Lasso regularization methods (Basu and Michailidis, 2015; Kock and Callot, 2015); forecast error variance decomposition (Diebold and Yilmaz, 2014); and Bayesian graph structural learning methods (Ahelegbey et al., 2016a,b; Carvalho and West, 2007). In this study, we derive the downside risk interconnectedness among stock markets via a Bayesian graph structural learning approach as in Ahelegbey et al. (2016a).

This paper relates to at least three streams of literature. The first is the network econometrics literature that applies network models to summarize contagion channels among financial institutions and markets using stock market data (Ahelegbey et al., 2016a; Billio et al., 2012; Diebold and Yilmaz, 2014). The second contribution relates to research on the impact of tail risk on asset returns (Ahelegbey et al., 2020; Almeida et al., 2017; Chabi-Yo et al., 2018; Harris et al., 2019; Mojtahedi et al., 2020; Van Oordt and Zhou, 2016). Van Oordt and Zhou (2016) studied a systematic tail risk measure that captures the sensitivity of asset returns to market returns conditional on market tail events. Almeida et al. (2017) analyzed a tail risk measure based on the risk-neutral excess expected shortfall of a cross-section of asset returns. Chabi-Yo et al. (2018) studied lower tail dependence (LTD) systematic tail risk based on estimating the sensitivity of an individual asset to a market crash. The third contribution relates to the application of the Bayesian graph-based network for estimating the downside risk interconnectedness.

We apply our proposed model to study the equities market by considering the 20 major stock market indices, selected for their market capitalization, covering countries across the Americas, Asia-Pacific, and Europe. The dataset consists of daily prices from Bloomberg, covering January 2000 to June 2020. The empirical application examines: 1) whether downside risk interconnectedness among the major stock markets are merely anecdotal or provide evidence of contagion, and 2) the most central market for spillover propagation. The result shows that periods of dense stock market downside risk interconnectedness increases global market risk. We find evidence that both transmitters and receivers of downside risk spillover propagation are mainly EU-centered markets.

The paper is organized as follows: Section 2 introduces the EDH model and the Bayesian graphical estimation method; Section 3 presents a description of the data; Section 4 reports the results; and Section 5 concludes the paper.

2. Methodology

In this section, we briefly describe the extreme downside hedge (EDH) technique for modeling downside risk sensitivity among assets. We also present the Bayesian and regularization techniques for constructing the downside risk interconnectedness among stock indices.

2.1. Extreme Downside Hedge (EDH) Model

The extreme downside hedge (EDH) model has in recent times been applied to study the sensitivity of returns to innovations in the tail risk of the market and/or of other counterparties (Ahelegbey et al., 2020; Harris et al., 2019; Mojtahedi et al., 2020). The EDH approach considered in this study is based on a well-known financial concept that in turbulent times some stock markets usually perform badly while others have mild reactions. Therefore markets that react mildly are often desirable. The variables of interest for the EDH model are the return series of stock markets and a measure of their downside (tail) risk. The commonly discussed measures for assessing the riskiness of assets/markets is the expected shortfall (also referred to as conditional value at risk - CoVaR/CVaR) (Adrian and Brunnermeier, 2016).

Let $Y_t = (Y_{1,t}, \ldots, Y_{n,t})$ be n-variable vector of return observations at time t, where $Y_{i,t}$ is the time series of asset-i at time t. Let $Y_{\tau,i}$ denote the left-side τ-quantile of the distribution on Y_i, for $\tau \in (0,1)$. Following Rockafellar and Uryasev (2002) and Gaivoronski and Pflug (2005), we compute the $CVaR_\tau(Y_i)$ as a proxy for the tail risk by

$$CVaR_\tau(Y_i) \;=\; \frac{1}{\tau}F_X(\tau)\; E\left(Y_i | Y_i < Y_{\tau,i}\right) + \left(1 - \frac{1}{\tau}F_X(\tau)\right) Y_{\tau,i} \tag{1}$$

where $F_X(\tau) = Pr(Y_i \leq Y_{\tau,i})$ is the cumulative density function (cdf) of Y_i. $CVaR_\tau(Y_i)$ calculates the weighted average of the losses that occur beyond $Y_{\tau,i}$, the value at risk point, in a distribution. We denote with $CVaR_{i,t}$, the $CVaR_\tau(Y_i)$ at time t. We employ $\Delta CVaR$ as a proxy for the innovation in the tail risk.

The return of an asset/stock can be influenced by the innovations in the tail risk of other asset/stocks that move with it. We model the sensitivity of the stock returns of market-i with respect to the innovation in the tail risk of other stock markets as

$$Y_{i,t} = \sum_{i \neq j = 1}^{n} B_{ij}\; \Delta CVaR_{j,t} + \varepsilon_{i,t} \tag{2}$$

where $\Delta CVaR_{j,t} = CVaR_{j,t} - CVaR_{j,t-1}$, B_{ij} is the sensitivity of the returns of market-i to the downside risk of market-j. The vector of error term $\varepsilon_t = (\varepsilon_{1,t}, \ldots, \varepsilon_{n,t})$ is assumed to be multivariate normal, $\mathcal{N}(0, \Sigma_\varepsilon)$.

2.2. Network (Graphical) Model

A network model is a convenient representation of the relationships among a set of variables. They are defined by nodes joined by a set of links, describing the statistical relationships between a pair of variables. The introduction of networks in regression models helps to interpret the predictor-dependent variable relationships. To analyze (2) through networks, we assign to each coefficient B_{ij} a latent indicator $G_{ij} \in \{0,1\}$, such that for $i, j = 1, \ldots, n$,:

$$B_{ij} = \begin{cases} 0 & \text{if} \;\; G_{ij} = 0 \;\; \Longrightarrow \;\; \Delta CVaR_{j,t} \;\not\to\; Y_{i,t} \\ \beta_{ij} \in \mathbb{R} & \text{if} \;\; G_{ij} = 1 \;\; \Longrightarrow \;\; \Delta CVaR_{j,t} \;\to\; Y_{i,t} \end{cases} \tag{3}$$

where $\Delta CVaR_{j,t} \not\rightarrow Y_{i,t}$ means that downside risk of market$-j$ does not influence the returns of market-i. Defining a sparse structure on (G, B) induces parsimony of the model and produces explainable downside risk models.

2.3. Bayesian Estimation Of Downside Risk Networks

Estimating network models have an intrinsic uncertainty with regards to the model structure and parameters, and it is well known that the number of valid configurations increases super-exponentially with the number of variables in the model. It is usually difficult to find one best network that can explain the data approximately well. In this study, we derive the downside risk interconnectedness among markets via a Bayesian graph structural learning approach as in Ahelegbey et al. (2016a).

2.3.1. Prior Specification

The objective of EDH network model is to estimate $(G, B, \Sigma_\varepsilon)$ using the available data. Estimating these parameters jointly is a challenging problem and a computationally intensive exercise for high dimensional models. We complete the Bayesian formulation with prior specification and posterior approximations to draw inference on the model parameters. We specify the prior distributions as follows:

$$[B_{ij}|G_{ij} = 1] \sim \mathcal{N}(0, \eta), \qquad G_{ij} \sim \text{Ber}(\pi_{ij}), \qquad \Sigma_\varepsilon^{-1} \sim \mathcal{W}(\delta, S_0) \tag{4}$$

where η, π_{ij}, δ, and S_0 are hyper-parameters. The specification for B_{ij} is conditionally Gaussian distributed with zero mean and variance η. Thus, relevant explanatory variables that predict a response variable must be associated with coefficients different from zero and the rest (representing not-relevant variables) are restricted to zero. We specify G_{ij} as Bernoulli distributed with π_{ij} as the prior probability, and consider Σ_ε^{-1} as Wishart distributed with prior expectation $\frac{1}{\delta}S_0$ and $\delta > n$ the degrees of freedom parameter. In this application, we set $\pi_{ij} = 0.5$ which leads to a uniform prior on the graph space, i.e., $P(G) \propto 1$. Following standard applications, we set $\eta = 100, \delta = n + 2$ and $S_0 = \delta I_n$.

2.3.2. Posterior Approximation

Let $Z_t = (\Delta CVaR_{j,1}, \ldots, \Delta CVaR_{j,n})$ be an $n \times 1$ vector of downside risk observations, denote with $Y = (Y_1, \ldots, Y_N)$ a $N \times n$ matrix collection of all return indices, and $Z = (Z_1, \ldots, Z_N)$ be an $N \times n$ matrix collection of Z_t. Let $V_y = (y_i, \ldots, y_n)$ be the vector of indices of response variables, and $V_z = (z_1, \ldots, z_n)$ the indices of the variables in Z. The network relationship from $z_\psi \in V_z$ to $y_i \in V_y$ can be represented by $(G_{y_i,z_\psi} = 1)$.

The Bayesian framework of Geiger and Heckerman (2002) can be applied to integrate out the structural parameters analytically to obtain a marginal likelihood function over graphs. The closed-form expression of the local marginal likelihood is given by

$$P(Y|G_{y_i,z_\psi}) = \frac{\pi^{-\frac{1}{2}N}}{\nu_n^{\frac{1}{2}\nu_n}} \frac{\nu_0^{\frac{1}{2}\nu_0}}{\Gamma\left(\frac{\nu_0 - n_x}{2}\right)} \frac{\Gamma\left(\frac{\nu_0 + N - n_x}{2}\right)}{\Gamma\left(\frac{\nu_0 - n_x}{2}\right)} \left(\frac{|Z_\psi' Z_\psi + \nu_0 I_{n_v}|}{|X_i' X_i + \nu_0 I_{n_x}|}\right)^{\frac{1}{2}\nu_n} \tag{5}$$

where $\Gamma(\cdot)$ is the gamma function, $X_i = (Y_i, Z_\psi)$, I_d is a d-dimensional identity matrix, n_ψ is the number of covariates in Z_ψ, $n_x = n_\psi + 1$, $\nu_0 > n_x$ is a degree of freedom hyper-parameter of the prior precision matrix of (Y, Z), and $\nu_n = \nu_0 + N$.

The above function allows us to apply an efficient Gibbs sampling algorithm to sample the graph structure in blocks (as in Roberts and Sahu, 1997). We approximate the graph and the parameters posterior distribution via a collapsed Gibbs sampler that proceeds as follows:

1. Sample via a Metropolis-within-Gibbs $[G|Y]$ (see Algorithm 1)
2. Sample from $[B, \Sigma_\varepsilon|Y, G]$ by iterating the following steps:
   (a) Sample $[B_{i,\pi_i}|Y, G, \Sigma_\varepsilon] \sim \mathcal{N}(\hat{B}_{i,\pi_i},\ D_{\pi_i})$ where

$$\hat{B}_{i,\pi_i} = \sigma_{u,i}^{-2} D_{\pi_i} Z'_{\pi_i} Y_i, \qquad D_{\pi_i} = (\eta^{-1} I_{d_z} + \sigma_{\varepsilon,i}^{-2} Z'_{\pi_i} Z_{\pi_i})^{-1} \tag{6}$$

   where $Z_{\pi_i} \in Z$ which corresponds to $(\hat{G}_{y_i,z_\pi} = 1)$, $\sigma^2_{\varepsilon,i}$ is the i-th diagonal element of $\hat{\Sigma}_\varepsilon$, and d_z is the number of covariates in Z_{π_i}.
   (b) Sample $[\Sigma_\varepsilon^{-1}|Y, G, B] \sim \mathcal{W}(\delta + N,\ S_N)$ where

$$S_N = S_0 + (Y - Z\hat{B}')'(Y - Z\hat{B}') \tag{7}$$

Algorithm 1 Sampling $[G|Y]$

Require: Set of responses $V_y = (y_i, \ldots, y_n)$ and predictor attributes $V_z = (z_1, \ldots, z_n)$
Initialize $G^{(1)} = \emptyset$
for $y_i \in V_y$ **do**
  for $z_j \in V_z$ **do**
    Compute $\phi_a = P(Y|G^{(1)}_{y_i,\emptyset})$ and $\phi_b = P(Y|G^{(1)}_{y_i,z_j})$
    if $\phi_b > \phi_a$ **then** $G^{(1)}_{y_i,z_j} = 1$ **else** $G^{(1)}_{y_i,z_j} = 0$
for $h = 2 : H$, (MCMC Iteration by performing local network update) **do**
  for $y_i \in V_y$, set $G^{(*)}_{y_i} = G^{(h-1)}_{y_i}$ **do**
    Randomly draw $z_k \sim V_z$
    Add/remove link from z_k to y_i: $G^{(*)}_{y_i,z_k} = 1 - G^{(h-1)}_{y_i,z_k}$
    Compute $\phi = \exp\,[\,\log P(Y|G^{(*)}_{y_i}) - \log P(Y|G^{(h-1)}_{y_i})\,]$. Draw $u \sim \mathcal{U}(0,1)$.
    if $u < \min\{1, \phi\}$ **then** $G^{(h)}_{y_i} = G^{(*)}_{y_i}$ **else** $G^{(h)}_{y_i} = G^{(h-1)}_{y_i}$

We examine the mixing of the chains generated by the Gibbs sampler for the samples of G. We monitor the mixing of the MCMC by computing the local log-likelihood score. We use the score to compute the potential scale reduction factor (PSRF) and multivariate PSRF (MPSRF) of Gelman and Rubin (1992). Following standard application, the MCMC chain is considered as converged if the PSRF and MPSRF are less than 1.2. With 50,000 sampled networks, we ensure that the convergence and mixing of the MCMC chains are tested with both PSRF and MPSRF satisfying the above condition.

We estimate the posterior probability of the edges by averaging over the sampled networks, i.e., $\hat{\gamma}_{ij} = \frac{1}{H}\sum_{h=1}^{H} G^{(h)}_{ij}$, where H is the total number of posterior samples of the graph. Due to the uncertainty in the network link determination, we consider a one-sided posterior credibility interval for the edge posterior distribution. Following Ahelegbey et al. (2016a), we parameterize the ij-th entry of the estimate of $\hat{G}$ via a link function:

$$\hat{G}_{ij} = \mathbf{1}(q_{ij} > 0.5), \qquad q_{ij} = \hat{\gamma}_{ij} - z_{(1-\alpha)}\sqrt{\frac{\hat{\gamma}_{ij}(1-\hat{\gamma}_{ij})}{n_{\text{eff}}}}, \qquad n_{eff} = \frac{H}{1 + 2\sum_{t=1}^{\infty}\rho_t} \tag{8}$$

where n_{eff} is the MCMC effective sample size of the network graph, ρ_t is the autocorrelation of the graph scores at lag t, and $z_{(1-\alpha)}$ is the z-score of the normal distribution at $(1-\alpha)$ significance level. A default value for α is 0.05 and $z_{(1-\alpha)} = 1.65$.

3. Data Description

Our study makes use of daily data from Bloomberg, covering between January 2000 to June 2020, and includes 15 major stock market indices, including all G10 economies. We consider only one index per country, which typically contains the stock prices of the largest companies listed in the nation's largest stock exchange. The countries can be grouped into three regions: the Americas (Brazil, Canada, Mexico, and the United States), Asia (China, Hong Kong, India, Japan, and South Korea), and Europe (France, Germany, Italy, Russia, Spain, and the United Kingdom). A description of the market indices chosen for the selected countries is presented in Table 1. The data cover January 3, 2000, to June 30, 2020.

Region	No.	Country	Code	Description	Index
Americas	1	Brazil	BR	Brazil Bovespa	IBOV
	2	Canada	CA	Canada TSX Comp.	SPTSX
	3	Mexico	MX	Mexico IPC	MEXBOL
	4	United States	US	United States S&P 500	SPX
Asia	5	China	CN	China SSE Comp.	SHCOMP
	6	Hong Kong	HK	Hong Kong Hang Seng	HSI
	7	India	IN	India BSE Sensex	SENSEX
	8	Japan	JP	Japan Nikkei 225	NKY
	9	Korea	KR	South Korean KOSPI	KOSPI
Europe	10	France	FR	France CAC 40	CAC
	11	Germany	DE	Germany DAX 30	DAX
	12	Italy	IT	Italy FTSE MIB	FTSEMIB
	13	Russia	RU	Russia MOEX	IMOEX
	14	Spain	ES	Spain IBEX 35	IBEX
	15	United Kingdom	UK	UK FTSE 100	UKX

Table 1: Detailed description of stock market indices of countries classified according to regions.

We report in Figure 1 the daily series of closing prices on a logarithmic scale. We scale the prices to a zero mean and unit variance and add the absolute minimum value of each series to avoid negative outcomes. This standardizes the scale of measurement for the different series. The figure shows that over the past two decades, global financial markets have experienced several catastrophic events within and across different markets. Among these events is 1) the dotcom "tech" and September 11 induced crisis of 2000–2003 which was fuelled by the adoption of the internet in the late 1990s, triggering inflated stock prices that gradually went downhill and disrupted global market operations; 2) the global financial crisis of 2007–2009 which was triggered by the massive defaults of sub-prime borrowers in the US mortgage market; 3) the European sovereign debt crisis of 2010–2013 which emanated from the inability of a cluster of EU member states to repay or refinance their sovereign debt and bailout heavily leveraged financial institutions without recourse to third party assistance; and 4) the ongoing distress to the world economy and global financial markets caused by the novel coronavirus pandemic in 2020.

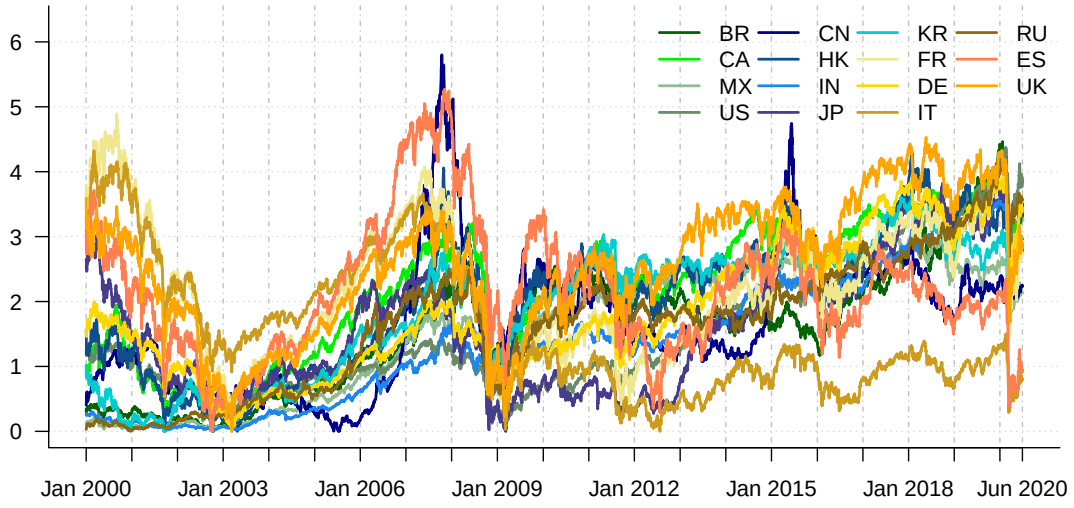

Figure 1: Daily closed prices of major stock market indices (January 3, 2000 – June 30, 2020).

We compute daily returns as the log differences of successive daily closing prices, that is, $Y_{i,t} = 100\,(\log P_{i,t} - \log P_{i,t-1})$, with $P_{i,t}$ the daily closing price of market i on trading day t. Table 2 reports a set of summary statistics for the index returns over the period from January 4, 2000 to June 30, 2020. From the summary statistics, we notice that almost all index returns

Country	Code	Mean	SD	Min	Max	Skew	Ex.Kurt
Brazil	BR	0.0330	1.8019	-15.9930	13.6783	-0.3833	6.8904
Canada	CA	0.0117	1.1381	-13.1758	11.2945	-0.9122	16.9927
Mexico	MX	0.0320	1.2745	-8.2673	10.4407	-0.0359	5.4752
United States	US	0.0145	1.2519	-12.7652	10.9572	-0.3683	11.2619
China	CN	0.0149	1.5213	-9.2561	9.4010	-0.3230	5.4697
Hong Kong	HK	0.0065	1.4394	-13.5820	13.4068	-0.1162	8.2032
India	IN	0.0358	1.4589	-14.1017	15.9900	-0.3454	9.6959
Japan	JP	0.0031	1.4659	-12.1110	13.2346	-0.3708	6.7584
Korea	KR	0.0137	1.4738	-12.8047	11.2844	-0.5658	7.4086
France	FR	-0.0035	1.4510	-13.0983	10.5946	-0.2163	6.2911
Germany	DE	0.0115	1.4902	-13.0549	10.7975	-0.1621	5.8342
Italy	IT	-0.0144	1.5436	-18.5411	10.8742	-0.5908	9.1267
Russia	RU	0.0553	1.9757	-20.6571	25.2261	-0.2033	16.5010
Spain	ES	-0.0091	1.4773	-15.1512	13.4836	-0.3162	7.9056
United Kingdom	UK	-0.0022	1.1950	-11.5117	9.3843	-0.3431	8.0884

Table 2: Statistics of daily returns for stock market indices (January 4, 2000 – June 30, 2020).

have a near-zero mean and a relatively high standard deviation, which ranges between 1.14 (Canada) and 1.98 (Russia). The highest standard deviations, indicating individual market volatilities, are those of the emerging markets of Russia and Brazil. The markets of Russia, Italy, and Brazil have the lowest minimum returns, while Russia, India, and Brazil have the highest maximum returns. The skewness of the returns ranges between -0.9122 (Canada) and -0.0359 (Mexico), indicating that all of them have fairly symmetric distributions with mostly small but consistent positive gains and, occasionally, large negative returns. The excess kurtosis varies between 5.470 (China) and 16.993 (Canada), which confirms the stylized facts

of leptokurtic behavior of daily return series.

We compute the daily $CVaR$ as in (1) via a 22-day horizon rolling estimation of daily returns. We used the Monte Carlo sampling approach to draw 1000 samples of the loss vector given the mean and standard deviation of the loss distribution. We replicate the simulation 10 times to estimate the $CVaR$ series. Table 3 reports the statistics for the daily $\Delta CVaR$ of the major stock market indices over the period from February 3, 2000, to June 30, 2020. From the Table 3, all the daily changes in the tail risk of the stock market returns have a zero

Country	Code	Mean	SD	Min	Max	Skew	Ex.Kurt
Brazil	BR	0.0004	0.2544	-3.0731	3.0865	-0.2242	28.9082
Canada	CA	0.0001	0.1747	-3.2112	2.1436	-1.0532	62.4697
Mexico	MX	0.0003	0.1769	-1.9235	1.3912	-0.3488	16.5186
United States	US	-0.0001	0.1787	-1.8684	2.5973	0.1191	27.8126
China	CN	0.0004	0.2471	-2.3572	2.6526	-0.1331	18.7071
Hong Kong	HK	0.0006	0.1998	-2.1350	2.3510	0.0941	20.2883
India	IN	0.0003	0.2220	-2.8665	3.1965	0.0254	43.3356
Japan	JP	-0.0002	0.2198	-2.8952	3.2137	-0.1819	32.0863
Korea	KR	0.0004	0.2260	-4.0167	3.4559	-0.5046	48.1533
France	FR	0.0000	0.2038	-2.6499	2.3645	-0.3510	24.9952
Germany	DE	-0.0000	0.2037	-3.0490	2.1356	-0.5367	24.4382
Italy	IT	-0.0002	0.2394	-4.4044	4.3535	-0.4472	81.1054
Russia	RU	0.0013	0.3039	-4.2120	3.3696	-0.8048	40.6139
Spain	ES	-0.0001	0.2271	-3.9767	4.4879	-0.0505	78.4251
United Kingdom	UK	0.0000	0.1685	-2.4683	1.8634	-0.4774	23.9300

Table 3: Statistics of daily $\Delta CVaR$ for stock market indices (February 3, 2000 – June 30, 2020).

mean and a relatively low standard deviation. Except for the US, Hong Kong, and India, which recorded fairly positive skewness, the rest have fairly negative symmetric distributions. The excess kurtosis confirms a leptokurtic behavior of daily changes in the tail risk.

4. Empirical Findings

We study the dynamics of the downside interconnectedness among the 15 major stock market indices via a yearly (approximately 240 trading days) rolling window. Our choice of window size is to capture the annual (12-months) dependence among the basis. We set the increments between successive rolling windows to one month. The first window covers February 2000 – January 2001, followed by March 2000 – February 2001, and the last from July 2019 – June 2020. In total, we have 234 rolling windows. First, we summarize the interconnectedness by studying the evolution of network density and market turbulence. We summarize the network topology via network centrality measures.

4.1. Network Density and Financial Market Risk

Here we address our first research question: Does downside risk interconnectedness among the major stock markets are merely anecdotal or provide evidence of contagion?

We characterize through numerical summaries the dynamic interconnectedness among the 15 major stock markets by monitoring the network density against the VIX index - a measure that reflects the market's expectation on the monthly volatility based on the S&P 500 index. Let G be an n-node unweighted adjacency matrix without self-loop. The network density is

given by the number of links in the estimated network divided by the total number of possible links. The network density is given by the number of links in the estimated network divided by the total number of possible links.

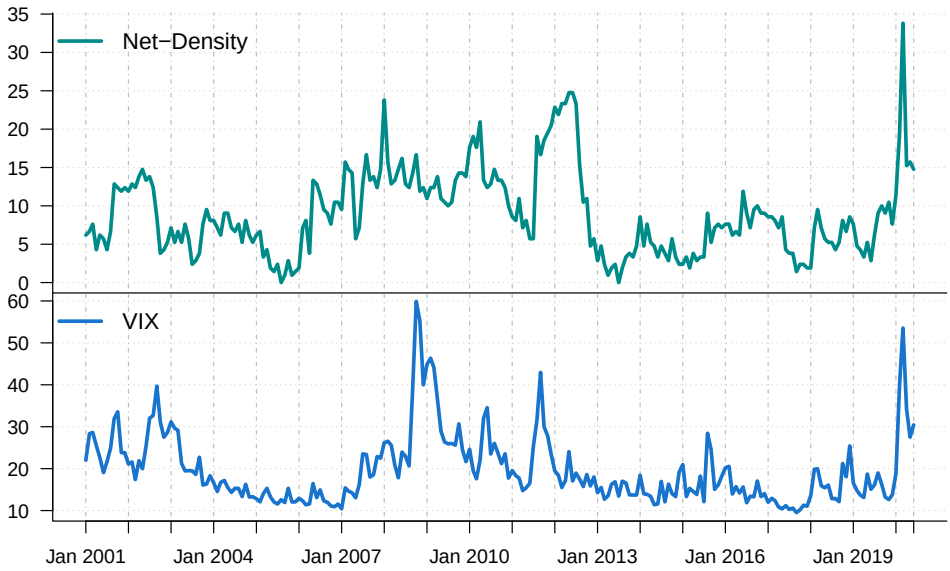

Figure 2: Network Density and VIX Index.

Figure 2 shows the time series of the network density against the VIX. The figure shows a strong positive relationship between Net-density and the VIX. Both indices indicate spikes during the tech-bubble crisis (2000–2003), the global financial crisis (GFC, 2007–2009), the Eurozone crisis (2010–2013), and the recent Covid-19 pandemic (2020:1H). The spikes in both indices at the onset of crisis periods indicate elevated levels of unusualness in the equity markets, a rise in financial market risk, and downside risk interconnectedness among stock markets. The historical highest Net-density recorded during the first half of 2020 shows that the COVID-19 induced downside risk exposure is much greater than any period of market crisis in the last 20 years.

In the interest of analyzing the relationship between downside risk interconnectedness and global market risk, we study the lead-lag relationship between the Net-Density and VIX. We stationarize each series via first differencing. Figure 3 presents the results of the cross-correlation of the first difference of Net-Density and VIX. The figure shows that the most

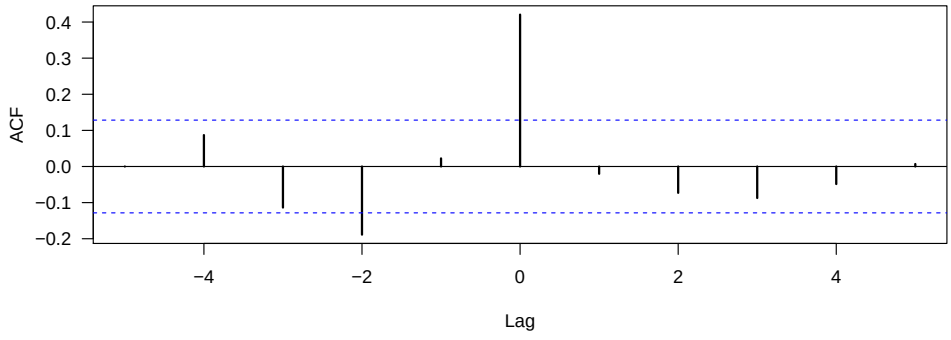

Figure 3: Correlation of ΔNet-Density$_{t+h}$ with ΔVIX$_t$.

significant cross-correlation between the Net-Density and the VIX occurs at lag 0. We also find evidence that the Net-Density preceded the VIX by 2-lags. This suggests that higher levels of downside risk interconnectedness preceded higher levels of financial market risk. Thus, the above findings show that the relationship between the network density of stock market downside risk interconnections and financial market risk is not a mere coincidence but rather evidence of contagion. That is, periods of dense stock market downside risk interconnectedness increases global market risk. This is in line with the findings of Billio et al. (2012) and Blume et al. (2013), among others, for which dense interconnectedness does amplify financial market risk.

4.2. Network Topology and Centrality

We turn our attention to the second research question: In the event of contagion, which stock market is central to downside risk propagation?

To address this question, we first analyze the topological structure of downside risk interconnectedness among the world stock markets. We divide the full sample into six sub-periods of tranquil (non-crisis) periods and turbulent times: (2001–2006), (2007–2009), (2010–2013), (2014–2016), (2017–2019) and 2020:1H. We report in Figure 4 the network topology over

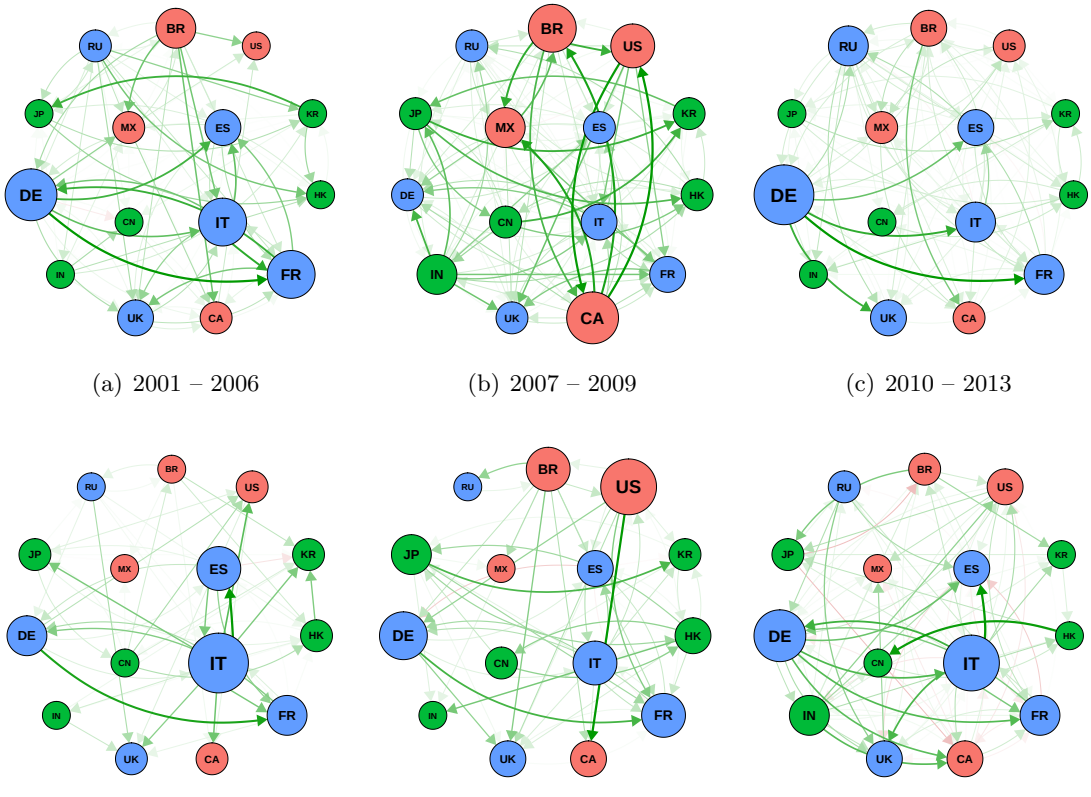

(a) 2001 – 2006 (b) 2007 – 2009 (c) 2010 – 2013

(d) 2014 – 2016 (e) 2017 – 2019 (f) 2020:1H

Figure 4: Sub-period networks. Red nodes denote markets in the Americas, blue for European countries, and green for Asian countries. The size of the nodes are based on a weighted out-degree.

the sub-periods. Each network is represented with color-coded links and nodes. Red-links indicate negative weights and green-links denote positive weights. Red-color nodes represent

American markets, blue-nodes for European markets, and green-nodes for markets in Asian countries. The size of the nodes is proportional to their hub scores. The links in the sub-period networks are predominately green suggesting a strong positive relationship between stock market returns and the downside risk of other markets.

We address the question of the most central market to downside risk propagation by studying node centrality of the networks. Commonly discussed centrality measures include in-degree (number of in-bounds links), out-degree (number of out-bound links), authority, and hub scores. The authority score of node-i is a weighted sum of the power/hub score of the vertices with directed links towards node-i. The hub score of node-j is the weighted sum of the power/authority score of vertices with a directed link from node-j. A hub node usually has a large out-degree and authority has a large in-degree. From a financial viewpoint, nodes with high authority scores/in-degree are highly influenced by others, while high hub scores/out-degree nodes are the influencers.

	Rank	Hub	Auth
Sub-Periods: Top Three Most Influential			
2001 – 2006	1	DE (0.345)	FR (0.360)
	2	IT (0.240)	ES (0.315)
	3	FR (0.229)	UK (0.300)
2007 – 2009	1	IN (0.253)	DE (0.381)
	2	BR (0.246)	UK (0.356)
	3	CA (0.217)	FR (0.347)
2010 – 2013	1	DE (0.526)	FR (0.372)
	2	BR (0.237)	UK (0.362)
	3	IT (0.204)	IT (0.268)
2014 – 2016	1	IT (0.470)	FR (0.294)
	2	ES (0.260)	KR (0.283)
	3	DE (0.156)	US (0.251)
2017 – 2019	1	US (0.315)	FR (0.392)
	2	BR (0.255)	UK (0.352)
	3	DE (0.227)	DE (0.247)
2020:1H	1	IT (0.492)	UK (0.434)
	2	DE (0.461)	ES (0.399)
	3	FR (0.280)	CA (0.386)
Full-Sample: Top Five Most Influential			
Core	1	DE (0.098)	FR (0.381)
	2	FR (0.011)	UK (0.345)
	3	IT (0.001)	ES (0.280)
	4	BR (0)	DE (0.232)
	5	CA (0)	IT (0.213)

Table 4: Centrality ranking of markets according to hub and authority scores.

Table 4 reports the centrality of the markets based on the median hub and authority scores. The table shows the top three ranked markets for the sub-periods and the top five over the full sample. Over the last two decades, Germany, France, and Italy are by far the most dominant markets in terms of stock market downside risk propagation according to the hub score ranking. Indeed, these European markets are integrated into Euronext - a

unique marketplace connecting many European economies. Thus, the most central markets to downside risk propagation are EU-centered markets, like Germany and France.

The authority score shows the most affected markets are France, the UK, Spain, Germany, and Italy. Again, these are European markets, which implies that the most affected markets as a result of downside risk spillover propagation are mainly also European-centered markets.

Overall, we observe that both the transmitters and receivers of downside risk spillover propagation are mainly European-centered markets that are integrated into Euronext.

5. Conclusion

This paper establishes the dynamic nature and extent of downside risk interconnectedness among major equity markets, including G10 economies. Our result shows strong evidence of tail risk interconnectedness among stock markets both in the tranquil period and during the crisis and post-crisis periods. We show that during crisis periods (when markets are more vulnerable), the degree of interconnectedness is particularly stronger and more persistent, which implies losses for investors already with long stock exposures. We also find that the level of downside risk spillovers induced by Covid-19 records the highest network density, suggesting stronger evidence of contagion in the recent coronavirus pandemic than during the global financial crisis and eurozone crisis. Central to the downside risk interconnectedness is the finding that most of the transmitters and recipients of tail risk spillovers propagate among EU-centered markets.

References

Adrian, T. and M. K. Brunnermeier (2016). CoVaR. *The American Economic Review 106*(7), 1705–1741.

Ahelegbey, D. F., M. Billio, and R. Casarin (2016a). Bayesian Graphical Models for Structural Vector Autoregressive Processes. *Journal of Applied Econometrics 31*(2), 357–386.

Ahelegbey, D. F., M. Billio, and R. Casarin (2016b). Sparse Graphical Vector Autoregression: A Bayesian Approach. *Annals of Economics and Statistics 123/124*, 333–361.

Ahelegbey, D. F. and P. Giudici (2020). Market Risk, Connectedness and Turbulence: A Comparison of 21st Century Financial Crises. *Available online: SSRN 3584510 (accessed on July 10, 2020)*.

Ahelegbey, D. F., P. Giudici, and F. Mojtahedi (2020). Tail Risk Measurement In Crypto-Asset Markets. *Available at SSRN 3556854 (accessed on 7/10/2020)*.

Almeida, C., K. Ardison, R. Garcia, and J. Vicente (2017). Nonparametric Tail Risk, Stock Returns and the Macroeconomy. *Journal of Financial Econometrics 15*(3), 333–376.

Basu, S. and G. Michailidis (2015). Regularized Estimation in Sparse High-dimensional Time Series Models. *The Annals of Statistics 43*(4), 1535–1567.

Battiston, S., D. Delli Gatti, M. Gallegati, B. Greenwald, and J. E. Stiglitz (2012). Liaisons Dangereuses: Increasing Connectivity, Risk Sharing, and Systemic Risk. *Journal of Economic Dynamics and Control 36*(8), 1121–1141.

Billio, M., R. Casarin, and L. Rossini (2019). Bayesian Nonparametric Sparse VAR Models. *Journal of Econometrics 212*(1), 97–115.

Billio, M., M. Getmansky, A. W. Lo, and L. Pelizzon (2012). Econometric Measures of Connectedness and Systemic Risk in the Finance and Insurance Sectors. *Journal of Financial Economics 104*(3), 535 – 559.

Blume, L., D. Easley, J. Kleinberg, R. Kleinberg, and É. Tardos (2013). Network Formation in the Presence of Contagious Risk. *ACM Transactions on Economics and Computation 1*(2), 6.

Carvalho, C. M. and M. West (2007). Dynamic Matrix-Variate Graphical Models. *Bayesian Analysis 2*, 69–98.

Chabi-Yo, F., S. Ruenzi, and F. Weigert (2018). Crash Sensitivity and the Cross Section of Expected Stock Returns. *Journal of Financial and Quantitative Analysis 53*(3), 1059–1100.

Diebold, F. and K. Yilmaz (2014). On the Network Topology of Variance Decompositions: Measuring the Connectedness of Financial Firms. *Journal of Econometrics 182*(1), 119–134.

Forbes, K. J. and R. Rigobon (2002). No Contagion, Only Interdependence: Measuring Stock Market Comovements. *The Journal of Finance 57*(5), 2223–2261.

Gaivoronski, A. A. and G. Pflug (2005). Value-at-Risk in Portfolio Optimization: Properties and Computational Approach. *Journal of Risk 7*(2), 1–31.

Geiger, D. and D. Heckerman (2002). Parameter Priors for Directed Acyclic Graphical Models and the Characterization of Several Probability Distributions. *Annals of Statistics 30*(5), 1412–1440.

Gelman, A. and D. B. Rubin (1992). Inference from Iterative Simulation Using Multiple Sequences, (with discussion). *Statistical Science 7*, 457–511.

Harris, R. D., L. H. Nguyen, and E. Stoja (2019). Systematic Extreme Downside Risk. *Journal of International Financial Markets, Institutions and Money 61*, 128–142.

Kock, A. B. and L. Callot (2015). Oracle Inequalities for High Dimensional Vector Autoregressions. *Journal of Econometrics 186*(2), 325–344.

Lauritzen, S. L. (1996). *Graphical Models*. Oxford University Press, Oxford.

Mendoza, E. G. and V. Quadrini (2010). Financial Globalization, Financial Crises and Contagion. *Journal of Monetary Economics 57*(1), 24–39.

Mojtahedi, F., S. M. Mojaverian, D. F. Ahelegbey, and P. Giudici (2020). Tail Risk Transmission: A Study of the Iran Food Industry. *Risks 8*(3), 78.

Roberts, G. O. and S. K. Sahu (1997). Updating Schemes, Covariance Structure, Blocking and Parametrization for the Gibbs Sampler. *Journal of the Royal Statistical Society 59*, 291 – 318.

Rockafellar, R. T. and S. Uryasev (2002). Conditional Value-at-Risk For General Loss Distributions. *Journal of Banking and Finance 26*(7), 1443–1471.

Van Oordt, M. R. and C. Zhou (2016). Systematic Tail Risk. *Journal of Financial and Quantitative Analysis 51*(2), 685–705.